Inorganic Chemistry

Article

pubs.acs.org/IC

New La(III) Complex Immobilized on 3-Aminopropyl-Functionalized Silica as an Efficient and Reusable Catalyst for Hydrolysis of Phosphate Ester Bonds

Alfredo A. Muxel,[†] Ademir Neves,*[,†] Maryene A. Camargo,[†] Adailton J. Bortoluzzi,[†] Bruno Szpoganicz,[†] Eduardo E. Castellano,[§] Nathalia Castilho,[#] Tiago Bortolotto,[#] and Hernán Terenzi[#]

[†]Departamento de Química, Laboratório de Bioinorgânica e Cristalografia (LABINC), Universidade Federal de Santa Catarina, SC, 88040-900 Florianópolis, Brazil

[§]Instituto de Física, Universidade Federal de São Carlos, São Carlos, SP 13560-970, Brazil

[#]Centro de Biologia Molecular Estrutural, Departamento de Bioquímica, Universidade Federal de Santa Catarina, SC, 88040-900 Florianópolis, Brazil

Supporting Information

ABSTRACT: Described herein is the synthesis, structure, and monoesterase and diesterase activities of a new mononuclear $[La^{III}(L^1)(NO_3)_2]$ (**1**) complex (H_2L^1 = 2-bis[{(2-pyridylmethyl)-aminomethyl}-6-[*N*-(2-pyridylmethyl) aminomethyl)]])-4-methyl-6-formylphenol) in the hydrolysis of 2,4-bis(dinitrophenyl)phosphate (2,4-BDNPP). When covalently linked to 3-aminopropyl-functionalized silica, **1** undergoes disproportionation to form a dinuclear species (**APS-1**), whose catalytic efficiency is increased when compared to the homogeneous reaction due to second coordination sphere effects which increase the substrate to complex association constant. The anchored catalyst **APS-1** can be recovered and reused for subsequent hydrolysis reactions (five times) with only a slight loss in activity. In the presence of DNA, we suggest that **1** is also converted into the dinuclear active species as observed with **APS-1**, and both were shown to be efficient in DNA cleavage.

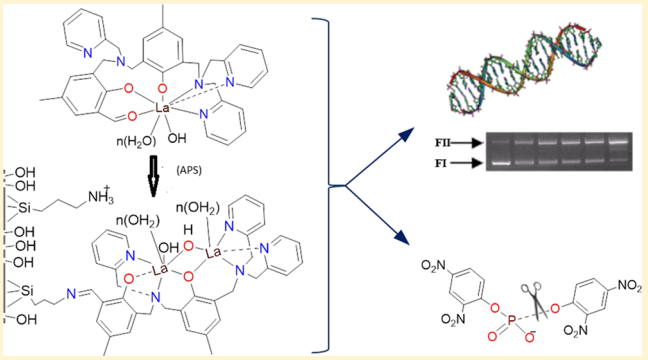

INTRODUCTION

The preparation of mono- and dinuclear metal complexes with catalytic activity as metallohydrolases and/or metalloproteases are nowadays common examples of synthetic bioinspired systems.[1] As the design of synthetic models becomes more effective, the use of such new compounds as catalysts, conformational probes, and synthetic restriction enzymes is expanding.[2] In this context, trivalent lanthanide ions display strong Lewis acidity, fast ligand-exchange rates, high coordination numbers, and an absence of accessible redox chemistry, which make them potential centers in the development of suitable artificial hydrolases.[3] In fact, Ln^{III} ions and their complexes have recently shown an extraordinary effect in accelerating the phosphate ester bond hydrolysis rate by several orders of magnitude.[4]

As one of many approaches to developing new useful catalysts, the immobilization of metal complexes onto the surface of insoluble solid matrices is an important tool promoting efficiency and selectivity of such materials.[5] Easy separation, efficient recycling of the catalyst, and the prevention of molecular aggregation or bimolecular self-destructive reactions are some advantages of such systems over homogeneous catalysis.[5] Studies on heterogeneous catalysts for the hydrolysis of phosphate diesters are relatively rare and, to the best of our knowledge, none of these involved lanthanides anchored to the silica surface.[6] On the other hand, methanolysis of neutral phosphate esters catalyzed by solid supported lanthanide ions have been reported.[7] Thus, we decided to carry out such studies based on our previous results.[8]

In this article, we report the synthesis, structure, and reactivity of a new mononuclear $[La(L^1)(NO_3)_2]$ (**1**) complex containing the unsymmetric ligand H_2L^1 (Chart 1), its attachment to 3-aminopropyl-functionalized silica gel (APS), and its activity toward the hydrolysis of the substrate 2,4-bis(dinitrophenyl)phosphate (2,4-BDNPP). Interestingly, our results indicate that this mononuclear complex disproportionates and that a dinuclear La^{III} species is formed when **1** is immobilized on the silica surface. This heterogeneous and reusable system presents higher catalytic efficiency compared to the homogeneous reaction.

Received: October 30, 2013
Published: March 3, 2014

   dx.doi.org/10.1021/ic402705r | *Inorg. Chem.* 2014, 53, 2943−2952

Chart 1. Unsymmetric Ligands H_2L and H_2L^1

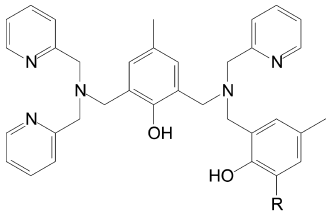

R = H (H_2L); R = CHO (H_2L^1)

EXPERIMENTAL SECTION

The abbreviations used are as follows: H_2L = 2-bis[{(2-pyridylmethyl)-aminomethyl}-6-{(2-hydroxybenzyl)-(2-pyridylmethyl)}aminomethyl]-4-methylphenol; HPNPP = hydroxypropyl-*p*-nitrophenyl phosphate; 2,4-BDNPP = 2,4-bis-(dinitrophenyl)phosphate; 2,4-DNPP = 2,4-(dinitrophenyl)-phosphate; 2,4-DNP = 2,4-dinitrophenolate.

Materials. The activated substrate 2,4-bis(dinitrophenyl)-phosphate was prepared as the pyridinium salt,[9] whereas the monoester 2,4-(dinitrophenyl)phosphate was obtained as the lutidinium salt.[10] The compound H_2L^1, which is 2-bis[{(2-pyridylmethyl)-aminomethyl}-6-[*N*-(2-pyridylmethyl) amino-methyl)]]-4-methyl-6-formylphenol, was prepared as described previously.[8] All other chemicals and solvents were of analytical or spectroscopic grade purchased from commercial sources and used without further purification.

Physical Measurements. Elemental analyses were performed on a Carlo Erba E-1110 instrument. IR spectra were recorded on a Perkin-Elmer model FTIR-2000 spectrometer, using KBr pellets, in the range of 4500−450 cm^{-1}. Electronic absorption spectra in the 200−1200 nm range were recorded on a Perkin-Elmer Lambda 750 spectrophotometer.

Electrospray ionization mass spectrometry (ESI-MS) of the complex dissolved in an ultrapure acetonitrile/water (1:1, v/v) solution (500 μL) was analyzed using an amaZon X Ion Trap MS instrument (Bruker Daltonics) with an ion spray source using electrospray ionization in positive-ion mode. The ion source condition was an ion spray voltage of 4500 V. Nitrogen was used as the nebulizing gas (20 psi) and curtain gas (10 psi). The samples were directly infused into the mass spectrometer at a flow rate of 300 μL/h. The scan range was m/z 200−3000.

X-ray Crystallography of Complex 1. The crystal was mounted on an Enraf-Nonius Kappa-CCD difractometer with graphite monochromated Mo Kα (λ = 0.71073 Å) radiation. The final unit cell parameters were based on all reflections. Data collections were made using the *COLLECT* program;[11] integration and scaling of the reflections were performed with the HKL Denzo-Scalepack system of programs.[12]

The structure was solved by direct methods with SHELXS-97,[13] the model was refined by full-matrix least-squares on F2 by means of SHELXL-97,[14] and all nonwater hydrogen atoms were placed at their calculated positions and refined with the riding model. There are two independent complexes in the asymmetric unit with coordination features similar to each other and to those previously reported, three disordered water molecules with occupancy 0.5, and four chloroform solvent molecules are present in the asymmetric unit. The H-atoms of the water molecule could not be found from the difference map. Selected crystallographic information is presented in Table 1, and full tables of crystallographic data (except structure factors) were deposited at Cambridge Structural

Table 1. Crystal Data and Structure Refinement for 1

empirical formula	$C_{38}H_{40}Cl_6LaN_7O_{10.5}$	
fw	1114.38	
temp	296(2) K	
wavelength	0.71073 Å	
cryst syst	triclinic	
space group	$P\bar{1}$	
unit cell dimensions	a = 9.8817(3) Å	α = 87.4220(10)°
	b = 14.9229(4) Å	β = 87.8130(10)°
	c = 34.1873(9) Å	γ = 71.724(2)°
vol	4780.7(2) $Å^3$	
Z	4	
density (calculated)	1.548 Mg/m^3	
abs coeff	1.289 mm^{-1}	
F(000)	2240	
cryst size	0.24 × 0.22 × 0.16 mm^3	
theta range for data collection	2.55 to 26.00°	
index ranges	$-12 \le h \le 8$, $-18 \le k \le 18$, $-42 \le l \le 42$	
reflns collected	47 252	
independent reflns	18 635 [R(int) = 0.0543]	
completeness to theta = 26.00°	99.1%	
abs correction	semiempirical from equivalents	
max and min transmission	0.8203 and 0.7472	
refinement method	full-matrix least-squares on F^2	
data/restraints/params	18 635/0/1153	
goodness-of-fit on F^2	1.043	
final R indices [I > 2sigma(I)]	R_1 = 0.0512, wR_2 = 0.1393	
R indices (all data)	R_1 = 0.0671, wR_2 = 0.1490	
largest diff. peak and hole	1.354 and −0.871 e.$Å^{-3}$	

dx.doi.org/10.1021/ic402705r | *Inorg. Chem.* 2014, 53, 2943−2952

Database (CCDC 968570) and are available free of charge at www.ccdc.cam.ac.uk.

Potentiometric Titrations. The potentiometric studies were carried out with a Corning-350 research pH meter fitted with blueglass and Ag/AgCl reference electrodes, in acetonitrile/water (50:50, v/v) solutions. The pK_a of the acetonitrile/water (50:50% v/v) containing 0.2 mol L^{-1} of KCl used was 15.40.[15] Equilibrium measurements were performed in a thermostatted cell, purged with argon, containing 50.00 mL of the acetonitrile/water (50:50) solution and 0.02 mmol of complex. The temperature was 25.00 ± 0.05 °C, and the experimental solutions were adjusted to 0.100 mol·L^{-1} of ionic strength by the addition of KCl. Computations of the triplicate results were carried out with the BEST7 program, and species diagrams were obtained with SPE and SPEPLO programs.[16]

Synthesis of the Complex $[La^{III}(L^1)(NO_3)_2]\cdot 3(CHCl_3)\cdot 1.5(H_2O)$ (1). Complex **1** was synthesized in methanolic solution by mixing $La(NO_3)_3\cdot 6H_2O$ and the ligand H_2L^1 (1:1 stoichiometry)[4] with stirring and mild heating (50 °C) for 30 min. After total evaporation of the solvent, the solid obtained was recrystallized through the slow diffusion of hexane in chloroform solution, yielding crystals suitable for X-ray analysis. The complex crystallizes as single yellow crystals that belong to the triclinic crystal system and space group $P\bar{1}$.

Yield: 75%. Anal. Calcd. for $C_{38}H_{40}Cl_6LaN_7O_{10.5}$: C, 40.96; H, 3.62; N, 8.80. Found: C, 41.02; H, 3.58; N, 8.87. Selected IR data (KBr): 3413, 1643, 1603, 1569, 1545, 1484, 1460, 1438, 1385, 1315, 1300, 1248, 1183, 1100, 1009, 864, 819, 796, 763, 729, 711 cm^{-1}.

Immobilization of 1 on 3-Aminopropyl-Functionalized Silica Gel. 3-Aminopropyl-functionalized silica gel (APS, 0.5 g) (Sigma-Aldrich; extent of labeling ~1 mmol/g NH2 loading, active group ~9% functionalized, matrix irregular silica particle platform, matrix active group NH2 phase, particle size of 40−63 μm, pore size of 60 Å, surface area of 550 m^2/g) was suspended in acetonitrile (10 mL) under mild magnetic stirring. Complex **1** (2.62×10^{-5} mol ≈22.4 mg) diluted in a minimal amount of acetonitrile was added. The mixture was stirred at room temperature for 24 h, and the solid was filtered and washed exhaustively with acetonitrile in a Soxhlet extractor for 12h. The supernatant solution was stored quantitatively to determine the amount of complex **1** immobilized on the support by comparison of the UV−vis absorption spectra obtained before and after immobilization. The color of the immobilized product became yellow and was finally dried under vacuum for 24 h. The material was designated as **APS-1** and was characterized by IR and UV−vis.

The amount of La(III) present in **APS-1** was analyzed by atomic absorption spectrometry, and this value was extrapolated to the concentration of the complex. The respective amount of **1** immobilized on **APS-1** was 5.08×10^{-5} mol/g APS (98%).

Immobilization of Ligand H_2L^1 on 3-Aminopropyl-Functionalized Silica Gel. The same method as described above was used with the ligand $\mathbf{H_2L^1}$ instead of **1**. The immobilized product was named $\mathbf{APS\text{-}L^1}$ (6.8×10^{-5} mol/g Si3AP) 86%.

Immobilization of $La(NO_3)_3\cdot 6H_2O$ on 3-Aminopropyl-Functionalized Silica Gel. The same method as described above was used with the salt $La(NO_3)_3\cdot 6H_2O$ instead of **1**. The immobilized product was named **APS-La** (1.78×10^{-5} mol/g Si3AP) 34%.

Reactivity Studies. Phosphatase-like activity of complex **1** was determined through the hydrolysis reaction of the model substrate bis(2,4-dinitrophenyl)phosphate (2,4-BDNPP) under substrate excess. The experiments were carried out, in triplicate, and monitored on a Varian Cary50 Bio spectrophotometer connected to a PC computer by following the increase in the 2,4-dinitrophenolate (DNP) characteristic absorption band at 400 nm (pH/ε L mol^{-1} cm^{-1} = (3.5/2125, 4.0/3408, 4.5/7182, 5.0/10078, 5.5/11405, 6.0/12004; 52 6.5−10.0/12100)[17] was followed. Reactions were monitored to less than 5% conversion of the substrate, and the data were treated using the initial rate method. Initial rates were obtained directly from the plot of the 2,4-dinitrophenolate concentration (2,4-DNP) versus time under the same experimental conditions.

In these experiments, all of the solutions were prepared in aqueous/buffer media, except the complex stock solution (3.0×10^{-4} mol L^{-1} in acetonitrile). Studies regarding the effects of pH on the hydrolysis reaction were performed in the pH range of 5.00−10.5 (MES pH 4.00−6.50; HEPES pH 7.00−8.50; CHES pH 9.00−10.5; I = 0.1 mol L^{-1} with $LiClO_4$), under a 50-fold excess of substrate at 25 °C. Experiments to determine the dependence of the reaction rate on the substrate concentration were carried out at 25 °C and pH 9.00 for both substrates (2,4-BDNPP and 2,4-DNPP). Spontaneous hydrolysis rate constants ($k_{uncat} = 1.78 \times 10^{-7}$ s^{-1} at pH = 6 and $k_{uncat} = 2.71 \times 10^{-7}$ s^{-1} at pH = 9) of the substrate bis(2,4-dinitrophenyl)phosphate (2,4-BDNPP) were obtained through the initial rate method.

Heterogeneous Reaction. In a typical reaction employing the heterogeneous catalyst, **APS-1** (2.4 mg, 1.22×10^{-7} mol) was weighed in a vial flask. The solid was suspended (1.5 mL of buffer and 1.4 mL of acetonitrile), and 0.1 mL of the substrate, 2,4- BDNPP, was added, resulting in a **APS-1**/substrate molar ratio of 1:50. The hydrolysis reaction was carried out during a controlled time interval (30 min) under magnetic stirring. The reaction product present in solution was separated from the solid catalyst by centrifugation, and the supernatant was analyzed by UV−vis. The same procedure was followed for control reactions using **APS** + 2,4-BDNPP substrate.

DNA Cleavage. The cleavage of DNA promoted by **1** and **APS-1** was evaluated analyzing the conversion of intact supercoiled form of pBSK II DNA (F I) to open circular (F II) and linear (F III) forms, which represent the plasmid forms containing single and double-strand breaks, respectively.[18] DNA cleavage reactions were conducted using 330 ng of pBSK II DNA (~25 μM in bp) in 10 mM of an appropriated buffer (MES, pH 5.5−6.0; HEPES, pH 7.0−8.0; and CHES, pH 9.0). The cleavage reaction was initiated by addition of the complexes (at different concentrations, depending of the assay) up to 24 h at 50 °C. At the end of reaction time, the mixtures were quenched by addition of a loading buffer solution (50 mM Tris-HCl pH 7.5, 0.01% bromophenol blue, 50% glycerol and 250 mM EDTA) and then subjected to electrophoresis on a 1.0% agarose gel containing 0.3 μg mL^{-1} of ethidium bromide in 0.5× TBE buffer (44.5 mM Tris, 44.5 mM boric acid and 1 mM EDTA at pH 8.0) at 90 V for 100 min. The resulting gels were visualized and digitized using a DigiDoc-It gel documentation system (UVP, U.S.A.). The proportion of plasmid DNA in each band was quantified using KODAK Molecular Imaging Software 5.0 (Carestream Health, U.S.A.). The quantitation of supercoiled DNA (F I) was corrected by a factor of 1.47, since the ability of ethidium bromide to intercalate into this DNA topoisomeric form is decreased

dx.doi.org/10.1021/ic402705r | Inorg. Chem. 2014, 53, 2943−2952

relative to open circular and linear DNA.[19] To verify the mechanism of DNA interaction and cleavage performed by the complexes, external agents were added to the reaction mixtures before each complex. These agents included NaCl (to increase the ionic strength of reaction media) and also different inhibitors of reactive oxygen species (ROS)[20], including DMSO (2 M), an $^{\bullet}OH$ scavenger KI (0.5 mM), which induces the disproportionation of peroxide-type species, and superoxide dismutase (SOD, 20 units), which scavenges $O_2^{\bullet-}$. In addition, some DNA groove binders were used in competition assays to determine the groove binding preference of the complexes: distamycin A (50 μM), which binds to the minor groove, and methyl green (50 μM), which binds to the major groove.

RESULTS AND DISCUSSION

Synthesis and X-ray Structure of Complex 1. Stoichiometric reaction of $La(NO_3)_3.6H_2O$ and the unsymmetric ligand H_2L^1 in methanolic solution results in the formation of the mononuclear $[La^{III}(L^1)(NO_3)_2]$ (**1**) complex. Suitable crystals for X-ray analysis were obtained through the slow diffusion of hexane in chloroform solution of **1**.

Complex **1** crystallized in a mononuclear form (Figure 1) and the main bond lengths and angles around the La^{III} center

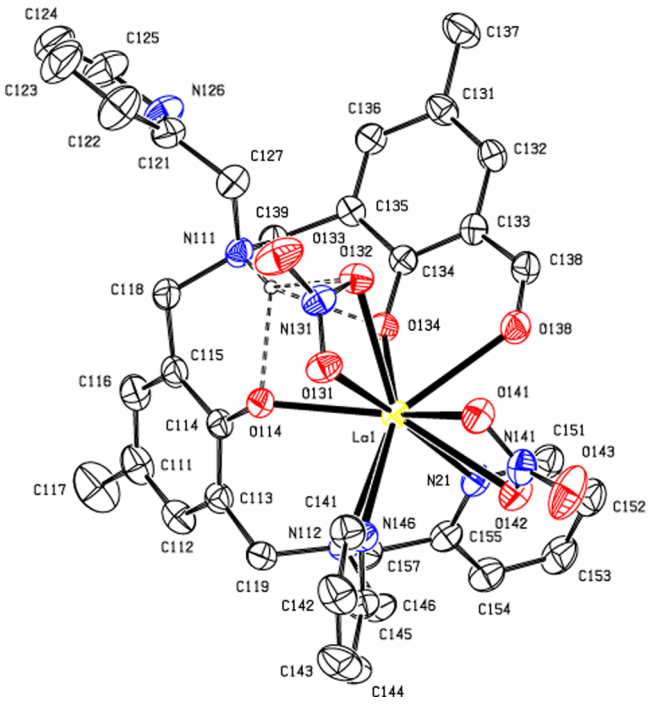

Figure 1. ORTEP plot of complex **1**.

are given in Table 2. The La^{III} metal ion is coordinated to the ligand L^1 through the nitrogen atom N112 of the tertiary amine (2.78 Å), two nitrogen atoms N146 and N21 of the pyridines (~2.79 Å), two oxygens O114 and O134 of the phenols (~2.40 Å), and one oxygen atom O138 of the aldehyde (2.67 Å). The La^{III} metal ion is also coordinated to the oxygen atoms of the bidentate nitrates (O131, O132 and O141, O142), thus completing its coordination sphere. The tertiary amine N111 is protonated and forms intramolecular hydrogen bonds involving the O114, O132, and O134 atoms and thus is not coordinated to the La^{III} center (see Table S1 in the Supporting Information). The bond lengths obtained are typical of La^{III}–phenolate bonds.[4b,21]

Immobilization of 1 on 3-Aminopropyl-Functionalized Silica Gel. Complex **1** and ligand H_2L^1 were covalently linked to 3-aminopropyl-functionalized silica gel (**APS-1** and **APS-L^1**), and these materials were analyzed by infrared (IR) (Figure 2 and Figure S1) and UV–vis (Figure 3) spectroscopies. The extent of immobilization of **1** and H_2L^1 on the surface of APS was determined by measuring the difference in absorbance values for a solution of the compound before and after addition of APS. Atomic absorption measurements were also performed to quantify the amount of bound complex (5.08×10^{-5} mol/g APS—98%).

After immobilization of the ligand and the complex **1**, the color of APS changed to yellow, which is characteristic of the ligand and complex **1** and the corresponding imine formation.

The IR spectrum of **APS-L^1** and **APS-1** contains broad and strong vibrational bands of Si–OH, Si–O, and Si–O–Si, typical of silica bonds that overlay the features corresponding to the ligand and complex **1**. The IR spectrum of APS shows a very broad band observed at 3700–3200 cm^{-1} due to the O–H stretching vibration of the hydroxyl groups. Another band at 1649 cm^{-1} is attributed to the H–O–H bending vibration of the adsorbed water. The strong band between 1200 and 1000 cm^{-1} and a band at 804 cm^{-1} are assigned to the Si–O–Si stretching vibrations. Furthermore, bands at 2925 and 2854 cm^{-1} due to CH_2 stretching vibrations of the propyl groups are also observed. On the other hand, the IR spectra of the immobilized systems compared to the aminopropyl silica is characterized by the appearance of new bands at 1600 to 1300 cm^{-1}, which is a strong indication of the immobilization of the ligand H_2L^1 and complex **1** on the silica surface (Figure 2, inset). In the case of **APS-1**, it is also possible to identify a band at 1385 cm^{-1}, which can be attributed to the stretching vibration of the coordinated nitrate in the immobilized complex.

The eletronic spectra of both the ligand H_2L^1 and complex **1**, in CH_3CN solution (Figure 3), exhibit strong absorptions at 290, 340, and 315, 390 nm (~4000 L mol^{-1} cm^{-1} per band), respectively, atributed to the intraligand $\pi \rightarrow \pi^*$ transitions in the phenolate and pyridine rings.[22] On the other hand, the electronic spectra of **APS-L^1** and **APS-1**, measured in the solid state (KBr pellets), exhibit absorption bands at 413 and 418 nm (Figure 3), absent in the ligand H_2L^1, which can be attributed to the imine chromophore formed by immobilizations of the ligand and complex **1** with the 3-aminopropyl group of APS.

Solution Studies: Potentiometric Titration and ESI-MS of 1. In order to establish the catalytically relevant species for the hydrolysis of diester bonds, potentiometric and ESI-MS studies of **1** were carried out in CH_3CN/water (1:1) solutions, the same solvent conditions as those employed for kinetic assays.

Potentiometric titrations of the ligand H_2L^1 and **1** in water/CH_3CN (1:1, v/v) were carried out in the pH range of 2–12. When **1** is dissolved in water/CH_3CN solution, the dissociation of the bound nitrates with replacement by water/CH_3CN molecules is expected and strongly supported by the ESI-MS data (vide infra). The equilibrium constants were determined for the complex as pK_{a1} = 5.5 attributed to the protonation/deprotonation equilibrium of the tertiary amine and pK_{a2} = 9.7 as being the result of the protonation/deprotonation equilibrium of a La^{III}-bound hydroxide (see Table S2 in the SI), and the values obtained were used to calculate the species

dx.doi.org/10.1021/ic402705r | Inorg. Chem. 2014, 53, 2943–2952

Table 2. Main Bond Distances (Å) and Angles (deg) for Complex 1

La1−O134	2.374(3)	La1−O131	2.727(3)
La1−O114	2.444(3)	La1−N112	2.784(4)
La1−O141	2.645(3)	La1−N146	2.787(4)
La1−O142	2.656(3)	La1−N21	2.810(4)
La1−O138	2.671(3)	La1−N141	3.065(4)
La1−O132	2.685(3)		
O134−La1−O114	75.96(11)	O138−La1−N112	135.77(11)
O134−La1−O141	132.67(11)	O134−La1−N146	158.48(12)
O134−La1−O142	127.83(11)	O114−La1−N146	85.65(11)
O134−La1−O138	67.24(10)	O138−La1−N146	133.91(11)
O114−La1−O138	137.12(10)	N112−La1−N146	60.58(12)
O134−La1−O131	111.88(10)	O134−La1−N21	76.13(11)
O134−La1−N112	102.43(11)	O114−La1−N21	116.46(11)
O114−La1−N112	72.19(11)	O138−La1−N21	75.76(12)
N112−La1−N21	60.10(12)	N146−La1−N21	102.97(12)
N112−La1−N141	103.42(12)	N146−La1−N141	64.62(12)
N21−La1−N141	86.78(12)		

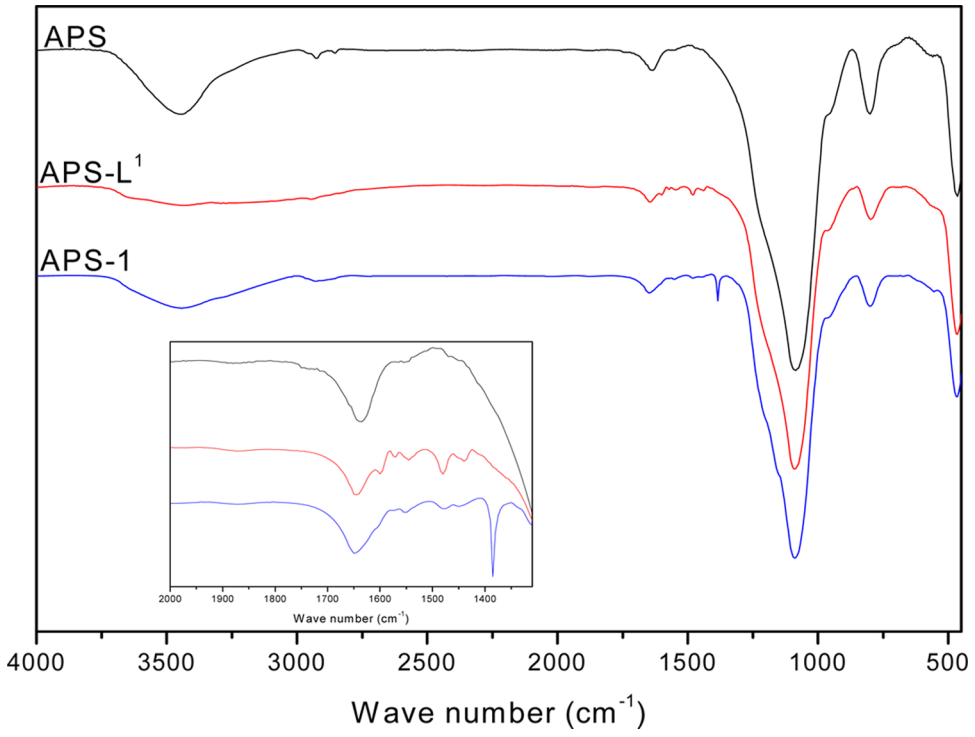

Figure 2. IR spectra of APS, **APS-L**[1], and **APS-1** (KBr pellet).

distribution curves (Figure 4). As can be observed in Figure 4, the percentage of the protonated amino species is very low (≈ 5%), because under these experimental pH conditions (pH < 5.0), the complex most probably dissociates into free ligand and the aqueous La^{III} ion.[4b] No binuclear complex was found to be formed in solution, and the species diagram obtained for mononuclear **1** correlates well with the catalytic activity as discussed below.

ESI-MS measurements for **1** in CH_3CN/H_2O (50:50,v/v) reveal a series of groups of peaks in the m/z 320 to 900 Da range, which are compatible with some degree of fragmentation of the complex (Figure 5 and Figure S2). The peaks observed at mass to charge m/z = 724.10 and 362.59 can be attributed to $[La(L^1)]^{1+}$ (E) and $[La(HL^1)]^{2+}$ (B), respectively, in which the NO_3^- ligands dissociate under the conditions of the electrospray ioinization, whereas the peak at m/z = 787.09 corresponds to the monocation $[La(HL^1)(NO_3)]^{1+}$ (F), in which one of the nitrates remains bound to the La^{III} ion. The peak observed at m/z = 860.26 is assigned to the $[La(L^1)(OH_2)_2(CH_3CN)_2]^+$ (G) species, indicating that solvent molecules are coordinated to the La^{III} center when **1** is dissolved in CH_3CN/H_2O (50:50). The group of peaks at mass to charge (m/z) ratios of 332.17 and 388.17 are assigned to the $[C_{21}H_{22}N_3O]^+$ (A) and $[C_{24}H_{24}N_2O_3]^+$ (C) species, which are derived from the fragmentation of L^1 (Figure S3), whereas the peak detected at m/z 588.28 corresponds to the protonated free ligand $[C_{36}H_{38}N_5O_3]^{1+}$ (D). Finally, it is important to emphasize that for **1**, there is no observation of dinuclear species under these conditions, in full agreement with the X-ray structural data and the proposed protonation/deprotonation equilibrium from potentiometric titration (vide supra). Thus, it is reasonable to conclude that in homogeneous solution, the

dx.doi.org/10.1021/ic402705r | Inorg. Chem. 2014, 53, 2943−2952

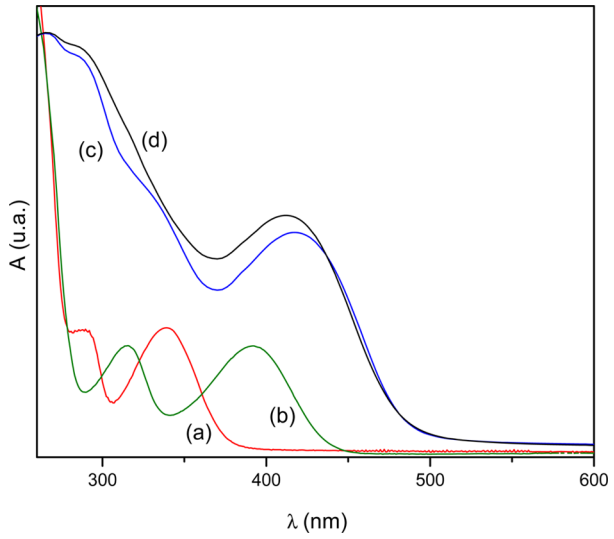

Figure 3. UV−vis spectra of (a) ligand H_2L^1 and (b) complex **1** in acetonitrile solution, (c) **APS-L^1**, and (d) **APS-1** in solid state (KBr pellet).

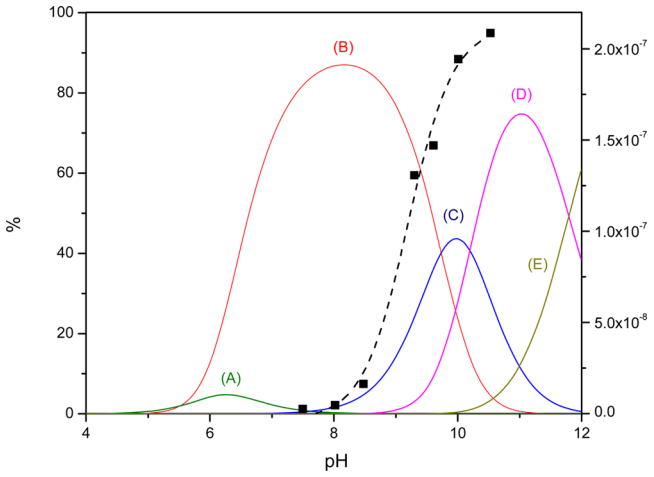

Figure 4. Solid lines represent the species distribution curves for **1** at 25 °C. The dashed line corresponds to the variation in the observed initial rates for the hydrolysis of 2,4-BDNPP as a function of pH in acetonitrile/water solution. Conditions: [**1**] = 4.0 × 10^{-5} mol L^{-1}; [2,4-BDNPP] = 2.0 × 10^{-3} mol L^{-1}; at 25 °C. (A) $[La(HL^1)]^{2+}$. (B) $[La(L^1)]^{1+}$. (C) $[La(L^1)(OH)]$. (D) $[La(L^1)(OH)_2]^{1-}$. (E) $[La(L^1)(OH)_3]^{2-}$.

mononuclear $[La(L^1)(OH)]$ structural unit is present as the catalytically active species in the hydrolysis of phosphate diester bonds (vide infra).

Hydrolase-Like Activity of 1 and APS-1. Homogeneous and heterogeneous kinetic experiments on the hydrolysis of the activated substrate 2,4-BDNPP by **1** and **APS-1** were carried out by monitoring the increase in the absorbance of the liberated 2,4-dinitrophenolate anion, under excess substrate at 25 °C and various pHs. The homogeneous catalytic activity of **1** was strongly influenced by the pH of the reaction mixture, as shown in the pH/rate profile curve in Figure 4. The curve was fitted using a Boltzman model to give a pK_a value of 9.2, which is in good agreement with the value (pK_{a2} = 9.6) obtained from the potentiometric titration experiments. These results strongly suggest that the $[La(L^1)(OH)]$ form of the complex is the catalytically active species in the 2,4-BDNPP cleavage. In order

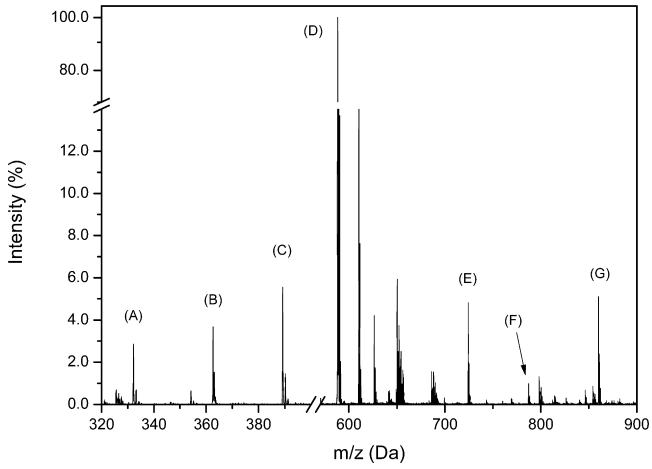

Figure 5. ESI-MS spectrum of **1** in CH_3CN/H_2O (1:1) solution. (A) *m/z* 332.17, $[C_{21}H_{22}N_3O]^+$. (B) *m/z* 362.59, $[C_{24}H_{24}N_2O_3]^+$. (C) *m/z* 388.17, $[C_{24}H_{24}N_2O_3]^+$. (D) *m/z* 588.28, $[C_{36}H_{38}N_5O_3]^{1+}$. (E) *m/z* = 724.10, $[La(L^1)]^{1+}$. (F) *m/z* = 787.09, $[La(HL1)(NO_3)]^{1+}$. (G) *m/z* 860.26, $[La(L^1)(OH_2)_2(CH_3CN)_2]^+$.

to confirm this hypothesis, kinetic studies on mixtures of $La(NO_3)_3.6H_2O$ and H_2L^1 (generated in situ) were carried out. As can be observed (Figure S4), the reaction reaches a maximum rate at the 1:1 mixture (La/**L^1**) and then remains almost unchanged in mixtures containing larger amounts of added metal (2.25:1), thus confirming the mononuclear complex $[La(L^1)(OH)]$ as being the catalytically active species in homogeneous media.

Measurements of the initial rates at pH 9.0 on increasing the substrate concentration (0.1−1.7 mmol L^{-1}) revealed saturation kinetics with Michaelis−Menten-like behavior (Figure S5 in the SI). Nonlinear regression was performed, and the calculated kinetic parameters are listed in Table 3. Under these experimental conditions, **1** displayed a 28 000-fold acceleration compared to the uncatalyzed hydrolysis (k_{uncat} = 2.71 × 10^{-7} s^{-1}).

Table 3. Kinetic Parameters for 2,4-BDNPP Hydrolysis Promoted by 1 and APS-1

catalyst	K_M (mM)	$k_{cat} \times 10^3$ (s^{-1})	k_{cat}/K_M (M^{-1} s^{-1})	f^c
1^a	5.53	7.57	1.37	28 000
APS-1^b	1.89	8.20	4.34	46 000

^{a}pH 9.0. ^{b}pH 6.0. $^c f = (k_{cat}/k_{uncat})$; k_{uncat} = 1.78 × 10^{-7} s^{-1} (pH 6.0) and 2.71 × 10^{-7} s^{-1} (pH 9.0) in experimental conditions.

The heterogeneous reactions using **APS-1** were performed under experimental conditions identical to those employed in homogeneous media using a reference reaction without addition of the catalyst as a blank. APS alone did not cleave the substrate under any circumstances while $La(NO_3)_3{\cdot}6H_2O$ in combination with APS shows only very low activity when compared to the catalytic system **APS-1** (Figure S6).

The dependence of the heterogeneous activity on pH was measured from pH 4 to 10.5, resulting (surprisingly) in a bell-shaped pH/rate profile with a pH optimum at 6.0 (Figure 6). These data were fitted to Eq. S1,[23] (see SI), which defined two pK_a values, 5.12 and 6.94, and suggest that the catalytically active species is of the type $[(OH)La^{III}(\mu{-}OH)La^{III}(OH_2)]$. The decrease in reactivity at pH > 6.0 most probably arises because of the presence of the fully deprotonated [(OH)-

dx.doi.org/10.1021/ic402705r | Inorg. Chem. 2014, 53, 2943−2952

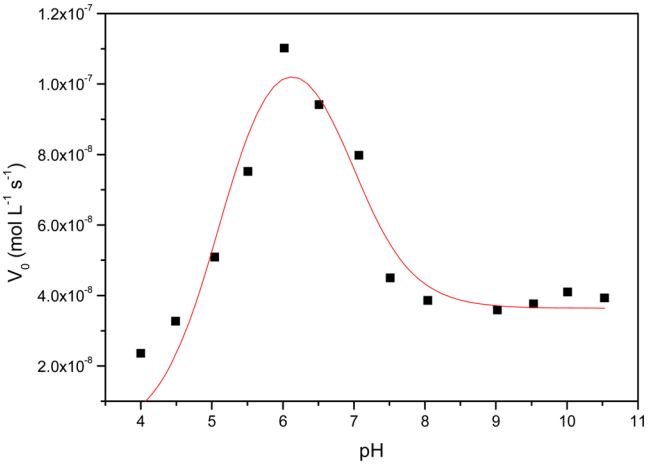

Figure 6. Dependence of the initial reaction rate (V_0) on pH for the hydrolysis of 2,4-BDNPP promoted by **APS-1**. Conditions: [**APS-1**] = 2.4 mg (4.0×10^{-5} mol L^{-1}); [2,4-BDNPP] = 2.0×10^{-3} mol L^{-1}; [buffers] = 50×10^{-3} mol L^{-1}; I = 50×10^{-3} mol L^{-1} (LiClO4) in H_2O/CH_3CN (50% v/v) at 25 °C.

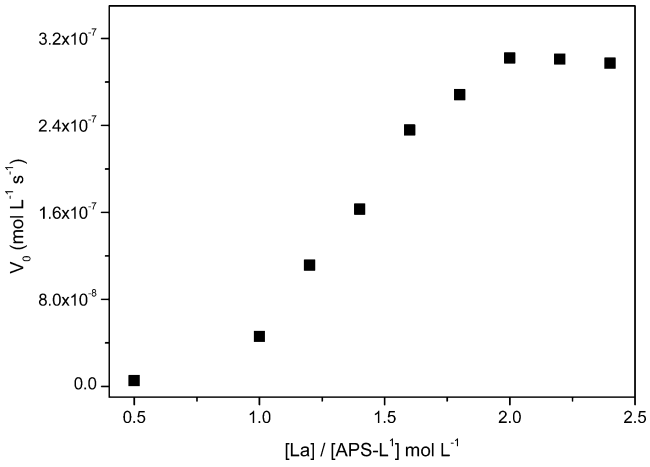

Figure 7. Dependence of the initial reaction rate (V_0) of 2,4-BDNPP on the ratio La(III)/APS-L^1. Conditions: [**APS-L^1**] = 5.44×10^{-5} mol/L; [La (III)] = 2.72×10^{-5} to 1.3×10^{-4} mol L^{-1}; [2,4-BDNPP] = 8.16×10^{-3} mol L^{-1}; pH = 6.0.

$La^{III}(\mu-OH)La^{III}(OH)]$ species in which the leaving tendency of the OH^- ion from the La−OH group becomes lower, even though a more concentrated OH^- solution can increase the spontaneous hydrolysis. Apparently, these results indicate that the reaction of the carbonyl group of L^1 (bound to the La^{III} center in the mononuclear complex **1**) with the amine of APS (Schiff base formation) seems to be necessary to disproportionate **1** and generate the dinuclear species. Moreover, such a conclusion is strongly supported by the fact that disproportionation of the mononuclear Gd^{III}, Tb^{III}, and Eu^{III} complexes containing the corresponding ligand L without the carbonyl attached to the terminal phenol group, occurs in the absence of a primary amine.[8b,24] Thus, despite the similarities of ligands L and L^1, the carbonyl attached to the terminal phenol group of L^1 induces the coordination of the La^{III} ion to the hard side of the unsymmetrical ligand due to the formation of the six-membered La−O−C−C−C-O−La ring with the carbonyl−phenolate chelate and stabilization of the mononuclear complex **1**.

As solution studies of **1** indicated a mononuclear complex as being the active complex in the catalysis (vide supra), kinetic studies were performed on mixtures of $La(NO_3)_3{\cdot}6H_2O$ and **APS-L^1** in order to obtain information on the species involved in the heterogeneous system. In the 1:1 mixture (La/**APS-L^1**), the catalytic activity of the system at pH = 6.0 toward the hydrolysis of 2,4-BDNPP is about 7×10^{-4} s^{-1} (Figure 7). However, when a 2:1 mixture (La/**APS-L^1**) was evaluated, the system had a maximum rate ($k_{obs} \cong 6 \times 10^{-3}$ s^{-1}) at the same pH observed in **APS-1**, this remaining unchanged in mixtures containing larger amounts of added metal. These results suggest that the 2:1 mixture provides, in situ, the formation of a binuclear complex that is 3 times more efficient as the homogeneous catalyst. Thus, these results lead to the proposal that disproportionation of the mononuclear complex **1** occurs along with binding to 3-aminopropyl silica (APS) to form a binuclear species and a free ligand.[24]

The determination of the initial rates as a function of the concentration of the substrate (0.05−1.7 mmol L^{-1}) also displays saturation kinetics with Michaelis−Menten-like behavior (Figure S7). A nonlinear fit resulted in the kinetic parameters presented in Table 3. The 2,4-BDNPP hydrolysis catalyzed by **APS-1** was 46 000 times faster than the spontaneous hydrolysis ($k_{uncat} = 1.78 \times 10^{-7}$ s^{-1}). The K_{ass} obtained ($K_{ass} \cong 1/K_M$) reveals greater stabilization of the substrate−catalyst intermediate in the heterogeneous system than in homogeneous media, although k_{cat} is only slightly higher, thus resulting in a catalytic efficiency which is ∼3 times higher for **APS-1**. The higher affinity of 2,4-BDNPP for the heterogeneous system **APS-1** presumably originates from some degree of influence of the solid support itself, because second sphere interactions with the substrate via hydrogen bonding, with the residual amino of 3-aminopropyl silica can occur.[8a] Nevertheless, it should be emphasized that under identical pH conditions (pH = 6.0, in which the **APS-1** system shows its maximum activity), the mononuclear complex is inactive and only the spontaneous hydrolysis of 2,4-BDNPP is detected. Thus at pH = 6.0 the dinuclear heterogeneous **APS-1** shows a catalytic activity which is about 48.000 times more effective than the mononuclear homogeneous complex **1**.

To assess the possible hydrolysis of the monoester 2,4-dinitrophenylphosphate (2,4-DNPP), one of the products formed from the hydrolysis reaction of the diester 2,4-BDNPP, a stoichiometric reaction between **1** or **APS-1** and 2,4-BDNPP was monitored. It was observed that 2 equiv of 2,4-DNP is released in 48 h for complex **1** and **APS-1** at 25 °C, which indicates a mono- and diesterase activity of the catalyst in the homogeneous and heterogeneous reactions. These results also suggest that the main product of the reaction, 2,4-dinitrophenolate, remains in solution, and no mass transfer at the interface of the heterogeneous catalyst occurs.[6b]

Hydrolysis experiments with 2,4-DNPP were conducted in a similar way to those for the diester 2,4-BDNPP. The homogeneous catalytic activity of **1** was very low, although it could be investigated in the presence of **APS-1**. The results are given in Figures S8 and S9. The kinetic parameters, $k_{cat} = 3.12 \times 10^{-4}$ s^{-1} and K_{ass}= 2451.0 mol^{-1} L, reveal that the association constant for the monoester and **APS-1** is around 4.6 times greater (bridging coordination is proposed in Scheme 1); however, k_{cat} is 13 times lower when compared to the parameters obtained with the corresponding 2,4-BDNPP diester. These data allowed us to conclude that distinct nucleophiles within **APS-1** act as the catalysts in the hydrolysis of the mono- and diester -phosphate substrates (Scheme 1) and

dx.doi.org/10.1021/ic402705r | Inorg. Chem. 2014, 53, 2943−2952

Scheme 1

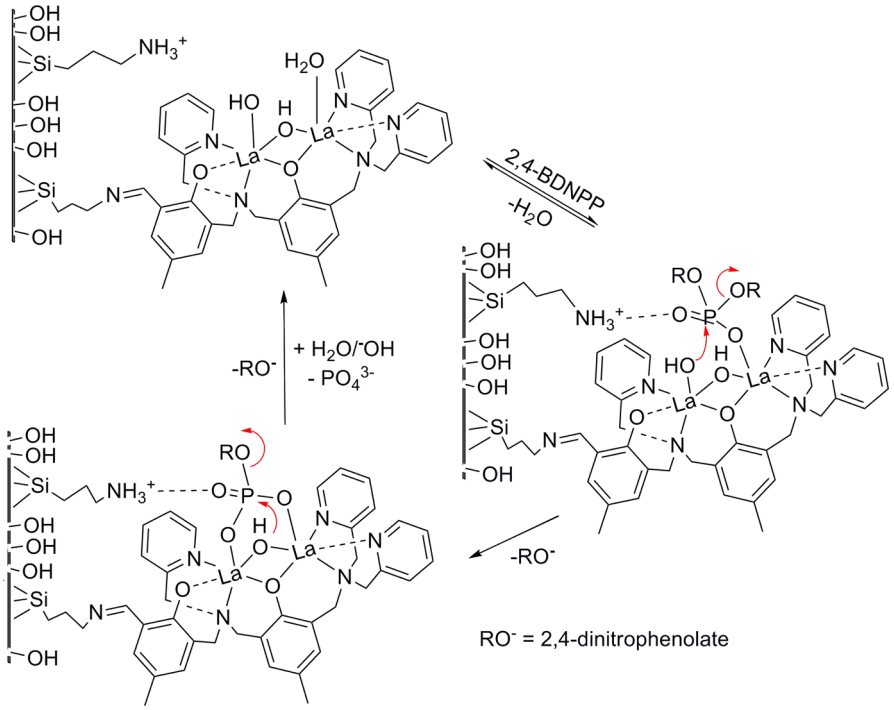

that the μ−OH is a significantly poorer nucleophile than the terminally La^{III}-bound OH^- group. Data from the literature, in which dinuclear $Ni^{II}Ni^{II}$ and $Fe^{III}Zn^{II}$ biomimetics and the enzyme $Fe^{III}Zn^{II}$ purple acid phosphatase have been used as the catalysts in the hydrolysis of mono- and diester-phosphate bonds are in full agreement with this proposal.[8,25,26]

For **1** and **APS-1**, 9 and 13 turnovers in 24 h were detected, providing evidence that during the catalytic cycle (excess of diester), the intermediate containing the monoester dissociates to regenerate the catalytically active species. Indeed, such a conclusion is reinforced by the fact that addition of 1 equiv of the monoester 2,4-DNPP (as a possible inhibitor) to the reaction mixture of **APS-1** and 2,4-BDNPP does not affect the number of turnovers in 24 h. Therefore, under excess substrate (2,4-BDNPP), hydrolysis of the monoester to form inorganic phosphate and 2,4-dinitrophenolate occurs mainly due to the background reaction (spontaneous hydrolysis). This conclusion is strongly corroborated by the fact that addition of one equiv of phosphate to the reaction mixtures significantly decreases the hydrolysis rate of 2,4-BDNPP (≈60%, with four and six turnovers for **1** and **APS-1**, respectively), thus suggesting that inorganic phosphate is a strong inhibitor which is formed only from the spontaneous hydrolysis of the monoester during the catalytic cycle. The isotopic effect was also evaluated, and the k_H/k_D ratios obtained for **1** and **APS-1** were 0.90 and 1.05 respectively. This corroborates the suggestion that the hydrolysis reaction of the diester 2,4-BDNPP proceeds through an intramolecular mechanism, in which the phosphorus atom undergoes a nucleophilic attack promoted by the La−OH group present in the active species.[25]

In summary, the combined data support the following mechanistic models in which the mononuclear $[La^{III}(L^1)(OH_2)(OH)]$ and dinuclear APS-$[(OH)La^{III}(\mu-OH)La^{III}(OH_2)]$ species of complex **1** are the catalytically relevant systems.

For the homogeneous system, the interaction of the substrate 2,4-BDNPP probably occurs by displacement of a coordinated H_2O or (CH_3CN) molecule prior to the intramolecular attack of the adjacent La^{III}-bound OH^- nucleophile leading to 2,4-dinitrophenolate and the intermediate in which the monoester is bonded to the La^{III} center. Under an excess of 2,4-BDNPP, we suggest that bonded phosphate monoester must be displaced by solvent molecules completing the catalytic cycle.

On the other hand, for the heterogeneous system, monodentate binding of 2,4-BDNPP by displacement of a La^{III}-coordinated H_2O molecule and activation via hydrogen bonding with the residual amino of 3-aminopropyl silica ($K_{ass} \cong 1/K_M$ = 530 M^{-1}) is followed by intramolecular nucleophilic attack by the terminal La^{III}-bound hydroxide and the concomitant release of 2,4-dinitrophenolate (Scheme 1). The μ-1,3 intermediate undergoes substitution by two water molecules and regenerates the catalytic dinuclear center for the next cycle. However, it is important to emphasize here that the stoichiometric reaction of **APS-1** and 2,4-BDNPP leads to the formation of 2 equiv of 2,4-dinitrophenolate, thus confirming that the monoester is also hydrolyzed under these experimental conditions, in agreement with the kinetic data obtained from the reaction of **APS-1** and the monoester 2,4-DNPP. Therefore, it seems reasonable to conclude that the monoester becomes activated by the two La^{III} centers (bridging coordination mode), and in principle, an intramolecular nucleophilic attack of the μ-hydroxide would be responsible for the hydrolysis of the bound monoester.

As reusability is of great interest for environmentally friendly heterogeneous catalysis, the catalyst was separated from the reaction mixture by simple filtration, washed in a Soxhlet extractor with 1:1 HEPES buffer at pH 6/acetonitrile, dried, and reused for the subsequent hydrolysis of 2,4-BDNPP. It could be observed that after the first reuse, the reaction rate decreased only 18% compared to the previous hydrolysis reaction (Figures S10 and S11), and for the third and

dx.doi.org/10.1021/ic402705r | Inorg. Chem. 2014, 53, 2943−2952

subsequent reuses, the reaction did not show a further significant reduction in the hydrolysis rate. The initial loss is probably caused by lixiviation of the supported catalyst due to imine hydrolysis or phosphate contamination.[8]

DNA Cleavage Activity. Additional assays were performed to verify the cleavage of a natural phosphate diester substrate, (i.e., DNA) by **1**. The first approximations revealed activity with a clear pH-dependence profile (Figure S12). A bell-shaped curve was obtained with optimum pH at around 7.0. In addition, the activity was found to be concentration-dependent, reaching ~80% of cleaved DNA after 16 h of reaction at 50 μM of **1** (Figure S13). Because the DNA molecule is negatively charged at pH 7.0, it is reasonable to believe that the electrostatic interactions between the complex and DNA could contribute to the binding and consequently to the cleavage event. To confirm this, DNA cleavage reactions were performed with increasing concentrations of NaCl (0.05 to 1 M) to modulate the ionic strength of the reaction media (Figure S14). The activity of the complex was strongly inhibited with increasing NaCl concentration. Sodium ions can be electrostatically attracted to the anionic portion of DNA, interfering with the interaction between the complex and DNA and preventing the cleavage. Further assays were performed to identify the dependence of reactive oxygen species (ROS) on the strand scission event, and as expected for lanthanide complexes,[3,4] the mechanism of DNA cleavage does not seem to proceed via an oxidative pathway (Figure S15). Also, the use of DNA groove binders to compete with **1** for DNA binding indicates that **1** may target both minor and major grooves (Figure S16). Lastly, the activity of **APS-1** toward the DNA substrate was determined and compared to the cleavage reaction promoted by **1** (Figure S17). **APS-1** could effectively cleave DNA in a similar fashion as **1**, but with a slightly lower cleavage yield (~80% for **1** vs ~50% for **APS-1**, after 24 h). We also verified that the pH-activity profile of **APS-1** is similar to that observed for **1**, with the activity being higher at pH 7.0 (Figure S18). These data suggest that under DNA cleavage reaction conditions, **1** and **APS-1** act as the binuclear species indicated in Scheme 1, suggesting that DNA can promote the disproportionation of the mononuclear complex, apparently by a similar pathway as described above for 3-aminopropyl-functionalized silica, where in this case, a nitrogen base (A, C, or G) could serve as a primary amine donor to form a Schiff base with **1**.

CONCLUSIONS

In summary, a new monocluclear La^{III} complex was covalently linked to solid supports containing primary amine functional groups. Kinetic studies indicated that the formation of a dinuclear complex attached to the solid surface of the APS increased the phosphatase-like activity, with high turnover rates in the hydrolysis of 2,4-BDNPP. The heterogeneous system presented higher catalytic efficiency (3 times higher than the soluble complex) due to the higher complex to substrate association constant. Also, **APS-1** can be reused for subsequent diester hydrolysis reactions. Finally, in the presence of DNA, **1** is apparently also converted into the dinuclear active species as **APS-1**, and both were shown to be efficient in DNA cleavage, which indicates their potential as artificial nucleases. Further studies involving the synthesis of the corresponding Gd^{III} and Tb^{III} complexes, their interaction with DNA, and their cytotoxic activity in adenocarcinoma cells are underway and will be the subject of future reports.

ASSOCIATED CONTENT

Supporting Information

X-ray crystallographic data in CIF format for **1**, synthesis and characterization of **1**, Tables S1−S2, and Figures 1, 5, S1−S18. The atomic coordinates for **1** have also been deposited with the Cambridge Crystallographic Data Centre as CCD 968570. The coordinates can be obtained, upon request, from the Director, Cambridge Crystallographic Data Centre, 12 Union Road, Cambridge CB2 1EZ, U.K. This material is available free of charge via the Internet at http://pubs.acs.org.

AUTHOR INFORMATION

Corresponding Author

*E-mail: ademir.neves@ufsc.br. Tel.: +55 (48) 3721-6844 R219.

Notes

The authors declare no competing financial interest.

ACKNOWLEDGMENTS

Financial support was received from CNPq, CAPES, FAPESC, INBEB, and INCT-catalise (Brazil).

REFERENCES

(1) (a) Desbouis, D.; Troitsky, I. P.; Belousoff, M. J.; Spiccia, L.; Graham, B. *Coord. Chem. Rev.* **2012**, *256*, 897. (b) Mitic, N.; Smith, S. J.; Neves, A.; Guddat, L. W.; Gahan, L. R.; Schenk, G. *Chem. Rev.* **2006**, *106*, 3338.

(2) Mancin, F.; Scrimin, P.; Tecilla, P. *Chem. Commun.* **2012**, *48*, 5545.

(3) Franklin, S. J. *Curr. Opin. Chem. Biol.* **2001**, *5*, 201.

(4) (a) Roigk, A.; Hettich, R.; Schneider, H.-J. *Inorg. Chem.* **1998**, *37*, 751. (b) Camargo, M. A.; Neves, A.; Bortoluzzi, A. J.; Szpoganicz, B.; Fischer, F. L.; Terenzi, H. A.; Serra, O. A.; Santos, V. G.; Vaz, B. G.; Eberlin, M. N. *Inorg. Chem.* **2010**, *49*, 6013. (c) Nwe, K.; Andolina, C. M.; Morrow, J. R. *J. Am. Chem. Soc.* **2008**, *130*, 14861. (c) Fanning, A. M.; Plush, S. E.; Gunnlaugsson, T. *Chem. Commun.* **2006**, 3791.

(5) Ohtaka, A. *Chem. Rec.* **2013**, *13*, 274.

(6) (a) Bodsgard, B. R.; Burstyn, J. N. *Chem. Commun.* **2001**, 647. (b) Zaupa, G.; Prins, L. J.; Scrimin, P. *Bioorg. Med. Chem. Lett.* **2009**, *19*, 3816. (c) Bodsgard, B. R.; Clark, R. W.; Ehrbar, A. W.; Burstyn, J. N. *Dalton Trans.* **2009**, 2365. (d) Rittich, B.; Španová, A.; Falk, M.; Beneš, M. J.; Hrubý, M. *J. Chromatogr. B* **2004**, *800*, 169. (e) Hanafy, A. I.; Lykourinou-Tibbs, V.; Bisht, K. S.; Ming, L.-J. *Inorg. Chim. Acta* **2007**, *358*, 1247. (f) Srivastan, S. G.; Parvez, M.; Verma, S. *Chem.—Eur. J.* **2002**, *8*, 5184.

(7) (a) Neverov, A. T.; Brown, R. S. *Ind. Eng. Chem. Res.* **2010**, *49*, 7027. (b) Neverov, A. T.; Brown, R. S. *Inorg. Chem.* **2001**, *40*, 3588.

(8) (a) Piovezan, C.; Jovito, R.; Bortoluzzi, A. J.; Terenzi, H.; Fischer, F. L.; Severino, P. C.; Pich, C. T.; Azzolini, G. G.; Peralta, R. A.; Rossi, L. M.; Neves, A. *Inorg. Chem.* **2010**, *49*, 2580. (b) Piovezan, C.; Silva, J. M. R.; Neves, A.; Bortoluzzi, A. J.; Haase, W.; Tomkowicz, Z.; Castellano, E. E.; Hough, T. C. S.; Rossi, L. M. *Inorg. Chem.* **2012**, *51*, 6104.

(9) Bunton, C. A.; Farber, S. J. *J. Org. Chem.* **1969**, *34*, 767.

(10) Rawji, G.; Milburn, R. M. *J. Org. Chem.* **1981**, *46*, 1205.

(11) Enraf-Nonius. *COLLECT*; Nonius BV: Delft, The Netherlands, 1997−2000.

(12) Otwinowski, Z.; Minor, W. In *Methods in Enzymology*; Carter, C.W., Jr., Sweet, R.M., Eds.; Academic Press: New York, 1997; Vol. *276*, pp 307−326.

(13) Sheldrick, G.M*SHELXS-97: Program for Crystal Structure Resolution*; University of Göttingen: Göttingen, Germany, 1997.

(14) Sheldrick, G.M *SHELXL-97: Program for Crystal Structures Analysis*; University of Göttingen: Göttingen, Germany, 1997.

(15) Herrador, M. A.; Gonzalez, A. G. *Talanta* **2002**, *56*, 769.

(16) Martell, A. E.; Motekaitis, R. J. *Determination and Use of Stability Constants*, 2nd ed.; VHC Publishers, Inc.: Weinheim, Germany, 1992.
(17) Batista, S. C.; Neves, A.; Bortoluzzi, A. J.; Vencato, I.; Peralta, R. A.; Szpoganicz, B.; Aires, V. V. E.; Terenzi, H.; Severino, P. C. *Inorg. Chem. Commun.* **2003**, *6*, 1161.
(18) (a) Neves, A.; Terenzi, H.; Horner, R.; Horn, A.; Szpoganicz, B.; Sugai, J. *Inorg. Chem. Commun.* **2001**, *4*, 388. (b) Scarpellini, M.; Neves, A.; Hörner, R.; Bortoluzzi, A. J.; Szpoganics, B.; Zucco, C.; Nome Silva, R. A.; Drago, V.; Mangrich, A. S.; Ortiz, W. A.; Passos, W. A. C.; De Oliveira, M. C. B.; Terenzi, H. *Inorg. Chem.* **2003**, *42*, 8353.
(19) Bernadou, J.; Pratviel, G.; Bennis, F.; Girardet, M.; Meunier, B. *Biochemistry* **1989**, *28*, 7268.
(20) (a) Bortolotto, T.; Silva, P. P.; Neves, A.; Pereira-Maia, E. C.; Terenzi, H. *Inorg. Chem.* **2011**, *50*, 10519. (b) Cavalett, A.; Bortolotto, T.; Silva, P. R.; Conte, G.; Gallardo, H.; Terenzi, H. *Inorg. Chem. Commun.* **2012**, *20*, 77. (c) Silva, P. P.; Guerra, W.; Silveira, J. N.; Ferreira, A. M. D. C.; Bortolotto, T.; Fischer, F. L.; Terenzi, H.; Neves, A.; Pereira-Maia, E. C. *Inorg. Chem.* **2011**, *50*, 6414.
(21) Xu, B.; Huang, L.; Yang, Z.; Yao, Y.; Zhang, Y.; Shen, Q. *Organometallics* **2011**, *30*, 3588.
(22) Neves, A.; Verani, C. N.; de Brito, M. A.; Vencato, I.; Mangrich, A.; Oliva, G.; Souza, D.; Batista, A. A. *Inorg. Chim. Acta* **1999**, *290*, 207.
(23) Smith, S. J.; Peralta, R. A.; Jovito, R.; Horn, A.; Bortoluzzi, A. J.; Noble, C. J.; Hanson, G. R.; Stranger, R.; Jayratne, V.; Cavigliasso, G.; Gahan, L. R.; Schenk, G.; Nascimento, O. R.; Cavalett, A.; Bortolotto, T.; Razzera, G.; Terenzi, H.; Neves, A.; Riley, M. J. *Inorg. Chem.* **2012**, *51*, 2065.
(24) Camargo, M. A.; Neves, A.; Bortoluzzi, A. J.; Szpoganicz, B.; Martendal, A.; Murgu, M.; Fischer, F. L.; Terenzi, H.; Severino, P. C. *Inorg. Chem.* **2008**, *47*, 2919.
(25) Neves, A.; Lanznaster, M.; Bortoluzzi, A. J.; Peralta, R. A.; Casellato, A.; Castellano, E. E.; Herrald, P.; Riley, M. J.; Schenk, G. *J. Am. Chem. Soc.* **2007**, *129*, 7486.
(26) Cox, R. S.; Schenk, G.; Mitic, N.; Gahan, L. R.; Hengge, A. C. *J. Am. Chem. Soc.* **2007**, *129*, 9550.